Continuous-variable quantum teleportation through lossy channels

A. V. Chizhov,* L. Knöll, and D.-G. Welsch
Theoretisch-Physikalisches Institut, Friedrich-Schiller-Universität Jena, Max-Wien-Platz 1, D-07743 Jena, Germany
(Received 4 June 2001; revised manuscript received 4 October 2001; published 10 January 2002)

The ultimate limits of continuous-variable single-mode quantum teleportation due to absorption are studied, with special emphasis on (quasi-) monochromatic optical fields propagating through fibers. It is shown that even if an infinitely squeezed two-mode squeezed vacuum were used, the amount of information that would be transferred quantum mechanically over a finite distance is limited and effectively approaches zero on a length scale that is much shorter than the (classical) absorption length. The state-dependent teleportation fidelity can be close to unity only for short distances. To realize the largest possibly fidelity, asymmetrical equipment must be used, where the source of the two-mode squeezed vacuum is nearer to Alice than to Bob and as a consequence the coherent displacement performed by Bob cannot be chosen independently of the transmission lengths.

DOI: 10.1103/PhysRevA.65.022310 PACS number(s): 03.67.−a, 42.50.Dv, 42.79.−e

I. INTRODUCTION

Quantum teleportation, in which an unknown quantum state is teleported from a sending station to a distant receiving station, has been one of the exciting manifestations of quantum-state entanglement of bipartite systems. Schemes for both spinlike quantum states [1,2] and continuous-variable quantum states [3–8] have been proposed, and experiments have been performed [9–12]. The very idea of quantum teleportation is to transfer that part of information on the (unknown) state which is lost in a single measurement quantum mechanically by means of appropriately entangled states.

In continuous-variable teleportation the sender (Alice) and the recipient (Bob) must share a highly entangled state in order to be able to really teleport an *arbitrary* quantum state. For teleporting a single-mode quantum state, a two-mode squeezed vacuum (TMSV) is commonly assumed to play the role of the entangled state. High entanglement then means high squeezing, which implies an entangled macroscopic (at least mesoscopic) state. However, entanglement is known to sensitively respond to environment influences, which unavoidably gives rise to entanglement degradation [13–15] and thus reduces the fidelity of teleportation, as was shown in Ref. [16], where the two modes were equally coupled to some heat bath.

The aim of the present paper is to study the ultimate limits of quantum teleportation that arise from absorption during the propagation of the two modes from the source of the TMSV to Alice and Bob, so that they have one each for further manipulation. Fibers are preferably used with regard to optical fields that are desired to propagate over longer distances. As we will see, the ratios of the propagation length to the low-temperature absorption length essentially determine the amount of quantum-mechanically transferable information. In this way, the fidelity of teleportation becomes not only state dependent, but also dependent on the position of the TMSV source relative to the positions of Alice and Bob. Thus, the original concept of teleportation of a really unknown quantum state to a really distant position becomes questionable.

The paper is organized as follows. Section II presents the basic equations, with special emphasis on the entangled state that is shared by Alice and Bob in practice and Bob's choice of the displacement after Alice's measurement. In Sec. III the theory is applied to the teleportation of squeezed states and number states and a detailed analysis of the various dependencies are given. Finally, some concluding remarks are given in Sec. IV.

II. BASIC EQUATIONS

In what follows we consider the standard scheme of continuous-variable single-mode teleportation, assuming the entangled state is a (strongly) squeezed TMSV. One mode is transmitted to Alice (sender) and the other one to Bob (recipient). Since the transmission, e.g., through fibers is unavoidably connected with some losses, the state effectively shared by Alice and Bob is not the originally generated TMSV but a mixed state, whose entanglement drastically decreases with the distance between Alice and Bob [17].

A. The teleported state

Let us briefly repeat the main stages of teleportation. If $W_{\rm in}(\gamma)$ is the Wigner function of the signal-mode quantum state that is desired to be teleported and $W^{\rm E}_{\rm out}(\alpha,\beta)$ is the Wigner function of the entangled state that is effectively shared by Alice and Bob, the Wigner function of the (three-mode) overall system then reads

$$W(\gamma,\alpha,\beta)=W_{\rm in}(\gamma)W^{\rm E}_{\rm out}(\alpha,\beta). \tag{1}$$

After combination of the signal mode and Alice's mode of the entangled two-mode system through a 50%:50% (lossless) beam splitter the Wigner function changes to

$$W(\mu,\nu,\beta)=W_{\rm in}\left(\frac{\mu-\nu}{\sqrt{2}}\right)W^{\rm E}_{\rm out}\left(\frac{\mu+\nu}{\sqrt{2}},\beta\right). \tag{2}$$

*Permanent address: Bogoliubov Laboratory of Theoretical Physics, Joint Institute for Nuclear Research, 141980 Dubna, Moscow Region, Russia.

Measurement of the real part of μ, μ_{R}, and the imaginary part of ν, ν_{I}, then prepares Bob's mode in a quantum state whose Wigner function is given by

$$W(\beta|\mu_{\mathrm{R}},\nu_{\mathrm{I}})=\frac{1}{P(\mu_{\mathrm{R}},\nu_{\mathrm{I}})}\int d\nu_{\mathrm{R}}\int d\mu_{\mathrm{I}}W_{\mathrm{in}}\left(\frac{\mu-\nu}{\sqrt{2}}\right)\times W_{\mathrm{out}}^{\mathrm{E}}\left(\frac{\mu+\nu}{\sqrt{2}},\beta\right), \tag{3}$$

where

$$P(\mu_{\mathrm{R}},\nu_{\mathrm{I}})=\int d\nu_{\mathrm{R}}\int d\mu_{\mathrm{I}}\int d^2\beta W(\mu,\nu,\beta) \tag{4}$$

is the probability density of measuring μ_{R} and ν_{I}. Introducing the complex variables

$$\gamma=(\mu-\nu)/\sqrt{2},\quad \gamma'=\sqrt{2}(\mu_{\mathrm{R}}-i\nu_{\mathrm{I}}), \tag{5}$$

we may rewrite Eq. (3) as

$$W(\beta|\gamma')=\frac{1}{P(\gamma')}\int d^2\gamma W_{\mathrm{in}}(\gamma)W_{\mathrm{out}}^{\mathrm{E}}(\gamma'^*-\gamma^*,\beta) \tag{6}$$

$[P(\mu_{\mathrm{R}},\nu_{\mathrm{I}})/2\rightarrow P(\gamma')]$.

Depending upon the result of Alice's measurement, Bob now coherently displaces the quantum state of his mode in order to generate a quantum state whose Wigner function is $W[\beta-\Delta(\gamma')|\gamma']$. If we are not interested in the one or the other measurement result, we may average over all measurement results to obtain the teleported quantum state on average:

$$W_{\mathrm{out}}(\beta)=\int d^2\gamma' P(\gamma')W[\beta-\Delta(\gamma')|\gamma'] =\int d^2\gamma W_{\mathrm{in}}(\gamma)\int d^2\gamma' W_{\mathrm{out}}^{\mathrm{E}}[\gamma'^*-\gamma^*,\beta-\Delta(\gamma')]. \tag{7}$$

B. Available entangled state

Let us assume that the modes of the originally generated TMSV propagate to Alice and Bob through fibers of (spectral) transmission coefficients $T_1(\omega)$ and $T_2(\omega)$, respectively. When

$$W_{\mathrm{in}}^{\mathrm{E}}(\alpha,\beta)=\frac{4}{\pi^2}\exp[-2(|\alpha|^2+|\beta|^2)\cosh|2\zeta| +2(e^{-i\varphi}\alpha\beta+e^{i\varphi}\alpha^*\beta^*)\sinh|2\zeta|] \tag{8}$$

is the Wigner function of the originally generated TMSV ($\zeta=|\zeta|e^{i\varphi}$, squeezing parameter), then the Wigner function of the quantum state, which the two modes are prepared in after transmission, takes the form of [13,15,18]

$$W_{\mathrm{out}}^{\mathrm{E}}(\alpha,\beta)=\frac{4}{\pi^2\mathcal{N}}\exp[-2(C_2|\alpha|^2+C_1|\beta|^2+S^*\alpha\beta +S\alpha^*\beta^*)], \tag{9}$$

where $(i=1,2)$

$$S=\frac{e^{i\varphi}}{\mathcal{N}}T_1T_2\sinh|2\zeta|, \tag{10}$$

$$C_i=\frac{1}{\mathcal{N}}[1+|T_i|^2(\cosh|2\zeta|-1)+2n_{\mathrm{th}\,i}(1-|T_i|^2)], \tag{11}$$

$$\mathcal{N}=[1+|T_1|^2(\cosh|2\zeta|-1)+2n_{\mathrm{th}\,1}(1-|T_1|^2)] \times[1+|T_2|^2(\cosh|2\zeta|-1)+2n_{\mathrm{th}\,2}(1-|T_2|^2)] -|T_1T_2|^2\sinh^2|2\zeta|, \tag{12}$$

with $n_{\mathrm{th}\,i}=\exp[\hbar\omega/(k_{\mathrm{B}}\vartheta_i)]-1\}^{-1}$ being the mean number of thermal excitations at temperature ϑ_i. It may be useful to express $|T_i|$ in terms of the ratio of the transmission length l_i to the absorption length $l_{\mathrm{A}\,i}$ such that

$$|T_i|=\exp(-l_i/l_{\mathrm{A}\,i}). \tag{13}$$

It should be pointed out that Eq. (9) together with Eqs. (10)–(12) directly follows from the general formalism of quantum-state transformation at absorbing four-port devices [19,20] for vanishing reflection coefficients. For nonvanishing reflection coefficients, the terms $n_{\mathrm{th}\,i}(1-|T_i|^2)$ in Eqs. (11) and (12) must be simply replaced with $n_{\mathrm{th}\,i}(1-|T_i|^2-|R_i|^2)$.

C. Fidelity

Let us assume that the quantum state to be teleported is a pure one, $\hat{\varrho}_{\mathrm{in}}=|\psi_{\mathrm{in}}\rangle\langle\psi_{\mathrm{in}}|$. A measure of how close to it is the (mixed) output quantum state $\hat{\varrho}_{\mathrm{out}}$ may be the teleportation fidelity

$$F=\langle\psi_{\mathrm{in}}|\hat{\varrho}_{\mathrm{out}}|\psi_{\mathrm{in}}\rangle. \tag{14}$$

Using the well-known representation of the density operator in terms of the coherent displacement operator $\hat{D}(\xi)$ [21,22],

$$\hat{\varrho}=\frac{1}{\pi}\int d^2\xi\chi(\xi)\hat{D}^{\dagger}(\xi), \tag{15}$$

with $\chi(\xi)$ being the Fourier transform of the Wigner function, Eq. (14) can be rewritten as

$$F=\frac{1}{\pi}\int d^2\xi\chi_{\mathrm{in}}(\xi)\chi_{\mathrm{out}}^*(\xi). \tag{16}$$

Equivalently, the fidelity can be given by the overlap of the Wigner functions:

$$F=\pi\int d^2\beta W_{\mathrm{in}}(\beta)W_{\mathrm{out}}(\beta). \tag{17}$$

Perfect teleportation implies unity fidelity; that is perfect overlap of the Wigner functions of the input and the output quantum state. Clearly, losses prevent one from realizing this case, so that the really observed fidelity is always less than unity. Thus, the task is to choose the scheme-inherent parameters such that the fidelity is maximized.

D. Choice of the displacement

An important parameter that must be specified is the displacement $\beta \to \beta - \Delta(\gamma')$ [in Eq. (7)], which has to be performed by Bob after Alice's measurement. For this purpose, we substitute Eq. (9) into Eq. (6) to obtain, on using the relation $C_1 C_2 - |S|^2 = \mathcal{N}^{-1}$,

$$W(\beta|\gamma') = \frac{1}{P(\gamma')} \frac{2}{\pi C_2 \mathcal{N}} \exp\left(-\frac{2}{C_2 \mathcal{N}} |\beta|^2 \right) \int d^2\gamma \frac{2C_2}{\pi} \times \exp\left(-2C_2 \left| \gamma' - \gamma + \frac{S^*}{C_2}\beta \right|^2 \right) W_{\rm in}(\gamma). \quad (18)$$

Here we have restricted our attention to optical fields whose thermal excitation may be disregarded ($n_{{\rm th}\,i} \approx 0$). From Eqs. (11) and (12) it follows that, for not too small values of the (initial) squeezing parameter $|\zeta|$, the variance of the Gaussian in the first line of Eq. (18), $C_2\mathcal{N}/4$, increases with $|\zeta|$ as $e^{2|\zeta|}|T_2|^2/8$, whereas the variance of the Gaussian in the integral in the second line, $1/(4C_2)$, rapidly approaches the (finite) limit ($T_2 \neq 0$)

$$\sigma_\infty = \lim_{|\zeta|\to\infty} \frac{1}{4C_2} = \frac{|T_1|^2 + |T_2|^2 - 2|T_1 T_2|^2}{4|T_2|^2}. \quad (19)$$

Thus, Bob's mode is prepared (after Alice's measurement) in a quantum state that is obtained, roughly speaking, from the input quantum state by shifting the Wigner function according to $\gamma \to \gamma' + \beta S^*/C_2$ and smearing it over an area whose linear extension is given by $2\sqrt{\sigma_\infty}$. It is therefore expected that the best that Bob can do is to perform a displacement with

$$\Delta(\gamma') = e^{i\tilde{\varphi}} \lambda \gamma', \quad (20)$$

where $\tilde{\varphi} = \varphi + \arg T_1 + \arg T_2$, and

$$\lambda = \lim_{|\zeta|\to\infty} \frac{C_2}{|S|} = \left| \frac{T_2}{T_1} \right|. \quad (21)$$

Substitution of this expression into Eq. (7) yields

$$W_{\rm out}(\beta e^{i\tilde{\varphi}}) = \frac{1}{2\pi\sigma\lambda^2} \int d^2\gamma W_{\rm in}(\gamma) \exp\left(-\frac{|\gamma - \beta/\lambda|^2}{2\sigma} \right), \quad (22)$$

where

$$\sigma = \frac{\mathcal{N}}{4\lambda^2}(C_2 + \lambda^2 C_1 - 2\lambda|S|). \quad (23)$$

Note that $\lim_{|\zeta|\to\infty} \sigma = \sigma_\infty$.

Clearly, even for arbitrarily large squeezing, i.e., $|\zeta| \to \infty$, and thus arbitrarily large entanglement, the input quantum state cannot be scanned precisely due to the unavoidable losses, which drastically reduce the amount of information that can be transferred nonclassically from Alice to Bob. Let δ_W be a measure of the (smallest) length scale in phase space on which the Wigner function of the signal-mode state, $W_{\rm in}(\gamma)$, typically changes. Teleportation then requires, apart from the scaling by λ, that the condition

$$\sigma_\infty \ll \delta_W^2 \quad (24)$$

is satisfied. Otherwise, essential information about the finer points of the quantum state are lost. For given δ_W, the condition (24) can be used in order to determine the ultimate limits of teleportation, such as the maximally possible distance between Alice and Bob. In this context, the question of the optimal position of the source of the TMSV arises. Needless to say, that all the results are highly state dependent.

III. SQUEEZED AND NUMBER STATES

Let us illustrate the problem for squeezed and number states. Applying the general formulas given in Sec. II to these classes of states, all calculations can be performed analytically and closed expressions for the fidelity can be derived. They will enable us to see the effect of the displacement and the position of the TMSV source in more detail.

A. Squeezed states

Let us first assume that the unknown single-mode quantum state, which is desired to be teleported, is a squeezed coherent state. Its Wigner function can be given by

$$W_{\rm in}(\gamma) = \frac{N_{\rm in}}{\pi} \exp[-A_{\rm in}|\gamma|^2 - B_{\rm in}(\gamma^2 + \gamma^{*}) + C_{\rm in}^{*}\gamma + C_{\rm in}\gamma^{*}], \quad (25)$$

where

$$N_{\rm in} = 2\exp[-2|\alpha_0|^2 \cosh(2\zeta_0) - (\alpha_0^2 + \alpha_0^{*2})\sinh(2\zeta_0)], \quad (26)$$

$$A_{\rm in} = 2\cosh(2\zeta_0), \quad (27)$$

$$B_{\rm in} = \sinh(2\zeta_0), \quad (28)$$

$$C_{\rm in} = 2[\alpha_0 \cosh(2\zeta_0) + \alpha_0^{*} \sinh(2\zeta_0)]. \quad (29)$$

Here, α_0 is the coherent amplitude and ζ_0 is the squeezing parameter, which is chosen to be real. Substituting Eq. (25) [together with Eqs. (26)–(29)] into Eq. (22), we derive (see the Appendix)

$$W_{\rm out}(\beta) = \frac{N_{\rm out}}{\pi} \exp[-A_{\rm out}|\beta|^2 - B_{\rm out}(\beta^2 + \beta^{*2}) + C_{\rm out}^{*}\beta + C_{\rm out}\beta^{*}], \quad (30)$$

where

$$N_{\rm out}=\frac{2}{\lambda^2\sqrt{1+8\sigma\cosh(2\zeta_0)+16\sigma^2}}\exp\left\{-\frac{2|\alpha_0|^2[\cosh(2\zeta_0)+4\sigma]+(\alpha_0^2+\alpha_0^{*2})\sinh(2\zeta_0)}{1+8\sigma\cosh(2\zeta_0)+16\sigma^2}\right\}, \tag{31}$$

$$A_{\rm out}=\frac{2[\cosh(2\zeta_0)+4\sigma]}{\lambda^2[1+8\sigma\cosh(2\zeta_0)+16\sigma^2]}, \tag{32}$$

$$B_{\rm out}=\frac{\sinh(2\zeta_0)}{\lambda^2[1+8\sigma\cosh(2\zeta_0)+16\sigma^2]}, \tag{33}$$

$$C_{\rm out}=2\frac{\alpha_0[\cosh(2\zeta_0)+4\sigma]+\alpha_0^*\sinh(2\zeta_0)}{\lambda[1+8\sigma\cosh(2\zeta_0)+16\sigma^2]} \tag{34}$$

($\tilde{\varphi}=0$). Combining Eqs. (17), (25)–(29), and (30)–(34), we arrive at the following expression for the fidelity (see the Appendix):

$$F\equiv F(\zeta_0,\alpha_0)=F(\zeta_0)\exp\left\{-\frac{(1-\lambda)^2}{2}\left[\frac{(\alpha_0+\alpha_0^*)^2e^{2\zeta_0}}{1+\lambda^2(1+4e^{2\zeta_0}\sigma)}-\frac{(\alpha_0-\alpha_0^*)^2}{(1+\lambda^2)e^{2\zeta_0}+4\lambda^2\sigma}\right]\right\}, \tag{35}$$

where

$$F(\zeta_0)=2[1+2\lambda^2+\lambda^4(1+16\sigma^2)+8\lambda^2(1+\lambda^2)\sigma\cosh(2\zeta_0)]^{-1/2} \tag{36}$$

is the fidelity for teleporting the squeezed vacuum.

From Eq. (35) it is seen that the dependence of F on α_0 vanishes for $\lambda=1$. Thus, the fidelity of teleportation of a squeezed coherent state can only depend on the coherent amplitude for an asymmetrical equipment (i.e., $|T_1|\neq|T_2|$). In this case, the fidelity exponentially decreases with increasing coherent amplitude. For stronger squeezing of the signal mode, the effect is more pronounced for amplitude squeezing [first term in the square brackets in the exponential in Eq. (35)] than for phase squeezing (second term in the square brackets).

In the case of a squeezed state, the characteristic scale δ_W in the inequality (24) is of the order of magnitude of the small semiaxis of the squeezing ellipse,

$$\delta_W\sim e^{-|\zeta_0|}. \tag{37}$$

For $|T_1|\approx|T_2|=|T|$, from Eqs. (19) and (37) it then follows that the condition (24) for high-fidelity teleportation corresponds to

$$1-|T|^2\ll e^{-2|\zeta_0|}, \tag{38}$$

that is,

$$\frac{l}{l_{\rm A}}\ll\ln(1-e^{-2|\zeta_0|})^{-1/2}. \tag{39}$$

Thus, for large values of the squeezing parameter $|\zeta_0|$, the largest teleportation distance that is possible, $l_{\rm T}$, scales as

$$l_{\rm T}\sim l_{\rm A}e^{-2|\zeta_0|}. \tag{40}$$

B. Number states

Let us now consider the case when the unknown quantum state is an N-photon number state. The input Wigner function then reads

$$W_{\rm in}(\gamma)=(-1)^N\frac{2}{\pi}\exp(-2|\gamma|^2)L_N(4|\gamma|^2) \tag{41}$$

[$L_N(x)$, Laguerre polynomial]. We substitute this expression into Eq. (22) and derive the Wigner function of the teleported state as

$$W_{\rm out}(\beta)=\frac{2}{\pi\lambda^2}\frac{(4\sigma-1)^N}{(4\sigma+1)^{N+1}}\exp\left[-\frac{2|\beta|^2}{\lambda^2(4\sigma+1)}\right]\times L_N\left[-\frac{4|\beta|^2}{\lambda^2(16\sigma^2-1)}\right]. \tag{42}$$

By combining Eqs. (17), (41), and (42), we then obtain the teleportation fidelity

$$F\equiv F_{\rm N}=2\frac{[\lambda^2(4\sigma-1)-1]^N}{[\lambda^2(4\sigma+1)+1]^{N+1}}\times{\rm P}_N\left\{1+\frac{8\lambda^2}{[\lambda^2(4\sigma+1)+1][\lambda^2(4\sigma-1)-1]}\right\} \tag{43}$$

[${\rm P}_N(x)$, Legendre polynomial].

From inspection of Eq. (41) it is clear that the characteristic length scale δ_W in the inequality (24) may be assumed to be of the order of magnitude of the (difference of two neighboring) roots of the Laguerre polynomial $L_N(x)$, which for large $N(N\gtrsim3)$ behaves like N^{-1} [23], thus

$$\delta_W\sim\frac{1}{\sqrt{N}}. \tag{44}$$

Assuming again $|T_1|\approx|T_2|=|T|$, the condition (24) together with Eq. (19) and δ_W^2 according to Eq. (44) gives

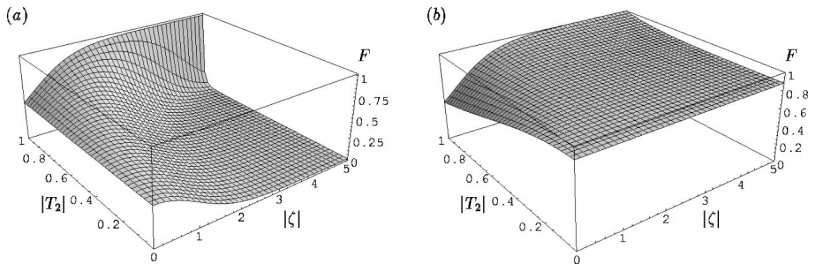

FIG. 1. The fidelity of teleportation of a squeezed vacuum state ($\zeta_0=0.5$) is shown as a function of $|\zeta|$ and $|T_2|$ ($|T_1|=1$, $\tilde{\varphi}=0$) for the displacement (a) $\Delta(\gamma')=\gamma'$ and (b) $\Delta(\gamma')=|T_2/T_1|\gamma'$ [Eqs. (20) and (21)].

$$1-|T|^2 \ll \frac{1}{N}. \tag{45}$$

It ensures that the oscillations of the Wigner function, which are typically observed for a number state, are resolved. Otherwise Bob cannot recognize the teleported state as an N-photon number state. Hence, the largest teleportation distance that is possible scales (for large N) as

$$l_{\mathrm{T}} \sim \frac{l_{\mathrm{A}}}{N}. \tag{46}$$

C. Discussion

Whereas for perfect teleportation, i.e., $|T_1|=|T_2|=1$, Bob has to perform a displacement $\Delta(\gamma')=e^{i\varphi}\gamma'$ [Eq. (20) for $\lambda=1$], which does not depend on the position of the source of the TMSV, the situation drastically changes for nonperfect teleportation. The effect is clearly seen from a comparison of Fig. 1(a) with Fig. 1(b). In the two figures, the fidelity for teleporting a squeezed vacuum state is shown as a function of the squeezing parameter $|\zeta|$ of the TMSV and the transmission coefficient $|T_2|$ for the case when the source of the TMSV is in Alice's hand, i.e., $|T_1|=1$. Figure 1(a) shows the result that is obtained for $\Delta(\gamma')=\gamma'$. It is seen that when $|T_2|$ is not close to unity, then the fidelity reduces, with increasing $|\zeta|$, below the classical level (realized for $|\zeta|=0$). In contrast, the displacement $\Delta(\gamma')=e^{i\tilde{\varphi}}\lambda\gamma'$ with λ from Eq. (21) ensures that the fidelity exceeds the classical level [Fig. 1(b)].

At this point the question may arise of whether the choice of λ according to Eq. (21) is the best one or not. For example, from an inspection of Eq. (18) it could possibly be expected that $\lambda=C_2/|S|$ also be a good choice. To answer the question, we note that in the formulas for the teleported quantum state and the fidelity, λ can be regarded as being an arbitrary (positive) parameter that must not necessarily be given by Eq. (21). Hence for a chosen signal state and given value of $|\zeta|$, the value of λ (and thus the value of the displacement) that maximizes the teleportation fidelity can be determined. Examples of the fidelity (as a function of $|\zeta|$) that can be realized in this way are shown in Fig. 2 for teleporting squeezed and number states according to Eqs. (35) and (43), respectively. The figure reveals that for not too small values of $|\zeta|$, that is, in the proper teleportation regime, the state-*independent* choice of λ according to Eq. (21) is indeed the best one.

After preparing this paper we have been aware of the article [24] in which it is argued that (even in the limit of infinite squeezing of the TMSV) the average coherent-state teleportation fidelity, which is obtained when integrating Eq. (35) ($\zeta_0=0$) over all coherent displacements α_0, is maximized for $\lambda=1$. This is certainly not correct. To see this, let us define the average fidelity more rigorously by introducing an appropriately chosen regularizing function,

$$\overline{F}=\frac{1}{\pi\overline{n}_{\mathrm{coh}}}\int d^2\alpha_0 F(\alpha_0)e^{-|\alpha_0|^2/\overline{n}_{\mathrm{coh}}} \tag{47}$$

[$F(\alpha_0)\equiv F(\zeta_0=0,\alpha_0)$ with $F(\zeta_0,\alpha_0)$ from Eq. (35)], and look (for chosen $|\zeta|$ and chosen ''cutoff'' coherent-photon

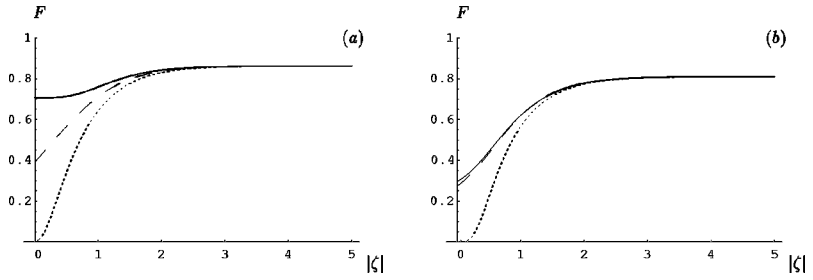

FIG. 2. The fidelity of teleportation of (a) a squeezed vacuum state ($\zeta_0=0.88$, i.e., $\overline{n}\approx 1$) and (b) a single-photon number state ($N=1$) is shown as a function of $|\zeta|$ ($|T_1|=1, |T_2|=0.9$, $\tilde{\varphi}=0$). The parameter λ in the displacement $\Delta(\gamma')=\lambda\gamma'$ is chosen such that maximum fidelity is realized. For comparison, the fidelities that are realized for $\lambda=|T_2/T_1|$ (dashed line) and $\lambda=C_2/|S|$ (dotted line) are shown.

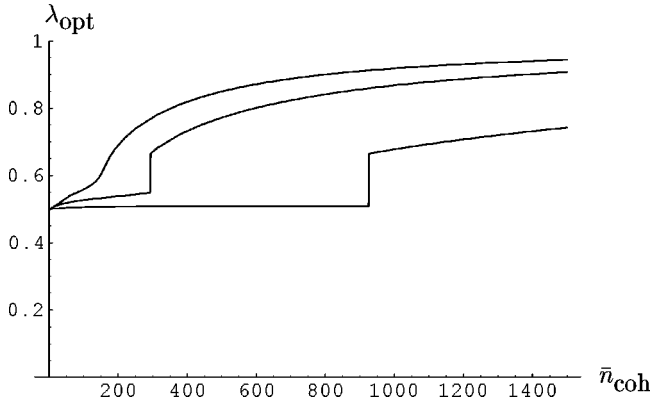

FIG. 3. The optimum displacement parameter for teleporting coherent states through asymmetrical equipment ($T_1=1$, $|T_2|=0.5$) is shown as a function of the cutoff coherent-photon number $\bar{n}_{\rm coh}$. The curves correspond to squeezing parameters $|\zeta|=3$ (upper curve), $|\zeta|=3.3$ (middle curve), and $|\zeta|=4$ (lower curve) of the initial TMSV.

number $\bar{n}_{\rm coh}$) for the value of λ that maximizes $\bar{F}$. Figure 3 shows the optimum displacement as a function of $\bar{n}_{\rm coh}$ for various values of $|\zeta|$ ($T_1=1$, $|T_2|=0.5$). One observes that for each value of $\bar{n}_{\rm coh}$ there exists always a (sufficiently large) value of $|\zeta|$ such that the optimum value of λ is exactly $|T_2/T_1|$. Thus, when performing the limits in the order required by quantum teleportation (first $|\zeta|\to\infty$, then $\bar{n}_{\rm coh}\to\infty$), the optimum displacement is always $\lambda_{\rm opt}=|T_2/T_1|$. Note that this is also valid when in Eq. (47) $F(\alpha_0)$ is replaced with $F(\zeta_0,\alpha_0)$ for arbitrary ζ_0. By the way, the average fidelity obtained in [24] is nothing but the fidelity for teleporting the vacuum, with displacement not properly chosen, i.e., $F(\zeta_0)$ from Eq. (35) for $\zeta_0=0$ and $\lambda=1$.

Figure 4 illustrates the dependence of the teleportation fidelity on the squeezing parameter $|\zeta|$ of the TMSV and the transmission coefficient $|T_2|$ ($|T_1|=1$) for squeezed and number states. It is seen that with increasing value of $|\zeta|$ the fidelity is rapidly saturated below unity, because of absorption. Even if the TMSV were infinitely entangled, the fidelity would be noticeably smaller than unity in practice. Only when $|T_2|$ is very close to unity, the fidelity substantially exceeds the classical level and becomes close to unity. (Note that the classical level is much smaller for number states than for squeezed states.) Hence, it seems to be principally impossible to realize quantum teleportation over distances that are comparable with those of classical transmission channels. The result is not unexpected, because the scheme is based on a strongly squeezed TMSV, which corresponds to an entangled *macroscopic* (at least *mesoscopic*) quantum state. Clearly, such a state decays very rapidly, so that the potencies inherent in it cannot be used in practice.

In order to illustrate the ultimate limits in more detail, we have plotted in Fig. 5, the dependence of the teleportation fidelity on the transmission length l_2 ($l_1=0$) for squeezed and number states, assuming an infinitely squeezed TMSV. It is seen that with increasing transmission length the fidelity decreases very rapidly, and it approaches the classical level on a length scale that is much shorter than the absorption length. In particular, the distance over which a squeezed state can really be teleported drastically decreases with increasing squeezing. Exactly the same effect is observed for number states when the number of photons increases. In other words, for a chosen distance, the amount of information that can be transferred quantum mechanically is limited, so that essential information about the quantum state that is desired to be teleported may be lost.

It may be interesting to compare the (maximally realizable) teleportation fidelity ($|\zeta|\to\infty$) with the classical level ($\zeta=0$). Figure 6 illustrates the dependence of the classical level on the transmission length l_2 ($l_1=0$) for the number states $|0\rangle,\ldots,|3\rangle$. For comparison, the average fidelity for the set of states is shown. With increasing transmission length the average fidelity rapidly approaches the classical level, i.e., the average of the classical levels of the set of states. In particular, it is seen that the long-distance average fidelity is substantially determined by the (classical level of the) vacuum teleportation. Clearly, the vacuum state is the only state that (for the chosen optimum displacement) can be teleported perfectly, without doing anything.

So far we have considered the extremely asymmetrical equipment where the source of the TMSV is in Alice's hand ($|T_1|=1$, i.e., $l_1=0$). Whereas for perfect teleportation the source of the TMSV can be placed anywhere, in practice the teleportation fidelity sensitively depends on the position of the source of the TMSV. In Fig. 7, examples of the optimal distance l_1 from Alice to the source of an infinitely squeezed TMSV (i.e., the distance for which maximum fidelity is realized) is shown, again for squeezed and number states, as a function of the distance $l_{12}=l_1+l_2$ between Alice and Bob. It is seen that the optimal position of the source of the TMSV is state dependent, and it is always nearer to Alice than to

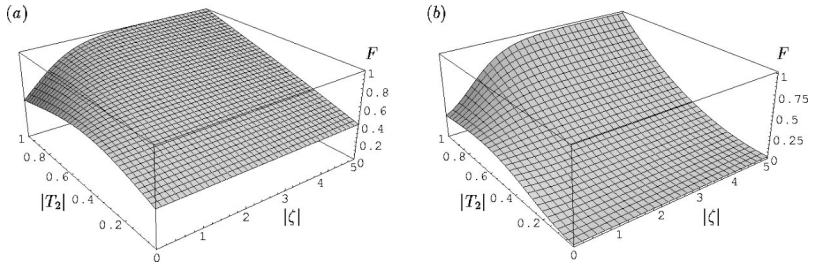

FIG. 4. The fidelity of teleportation of (a) a squeezed coherent state ($\zeta_0=0.5$, $\alpha_0\approx 0.7$, i.e., $\bar{n}\approx 1$) and (b) a single-photon number state ($N=1$) is shown as a function of $|\zeta|$ and $|T_2|$ ($|T_1|=1$, $\tilde{\varphi}=0$, $\lambda=|T_2/T_1|$).

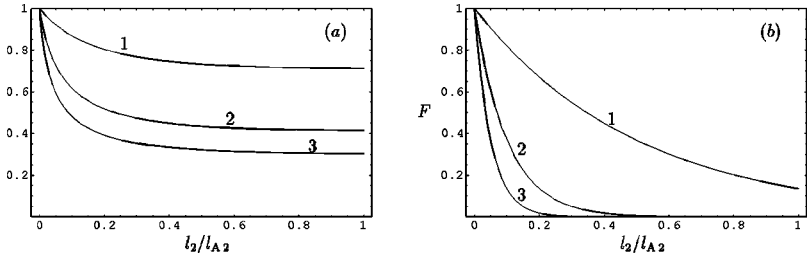

FIG. 5. The fidelity of teleportation of (a) squeezed vacuum states (curve 1: $\zeta_0=0.88$, i.e., $\bar{n}\approx 1$; curve 2: $\zeta_0=1.54$, i.e., $\bar{n}\approx 5$; curve 3: $\zeta_0=1.87$, i.e., $\bar{n}\approx 10$) and (b) number states (curve 1: $N=1$; curve 2: $N=5$; curve 3: $N=10$) is shown as a function of the transmission length l_2 for $|\zeta|\to\infty$ [$l_1=0$, $\tilde{\varphi}=0$, $\lambda=|T_2/T_1|=\exp(-l_2/l_{A2})$].

Bob ($0\leqslant l_1<0.5\,l_{12}$). With increasing value of l_{12} the value of l_1 approaches $0.5\,l_{12}$, and one could thus think that symmetrical equipment would be the best one. Unfortunately, this is not the case, because the transmission lengths are essentially too large for true quantum teleportation. What were (optimally) observed would be the classical level at best.

IV. SUMMARY AND CONCLUSIONS

In continuous-variable single-mode quantum teleportation it is commonly assumed that Alice and Bob share a strongly squeezed TMSV. We have analyzed this scheme, with special emphasis on the absorption losses that are unavoidably associated with the transmission of the two modes over finite distances, e.g., by means of fibers. In particular, we have applied the general formulas derived to the problem of teleporting squeezed states and number states, which are typical examples of nonclassical states.

The results show that the TMSV state as an effectively macroscopic (at least mesoscopic) entangled quantum state rapidly decays, and thus proper quantum teleportation is only possible over distances that are much shorter than the (classical) absorption length. Rapid decay of the TMSV state means that there is a strong entanglement degradation which dramatically limits the amount of information that can be transferred quantum mechanically over longer distances. Because of this limitation, quantum teleportation becomes state dependent, that is, without additional knowledge of the state that is desired to be teleported over some finite distance it is principally impossible to decide whether the teleported state is sufficiently close to the original state. Clearly, this contradicts the basic idea of quantum teleportation. It is worth noting that both the coherent displacement that must be performed by Bob and the position of the source of the TMSV should not be chosen independently of the fiber lengths. In particular, asymmetrical equipment, where the source of the TMSV is placed nearer to Alice than to Bob, is suited for realizing the largest possible teleportation fidelity and not a symmetrical one.

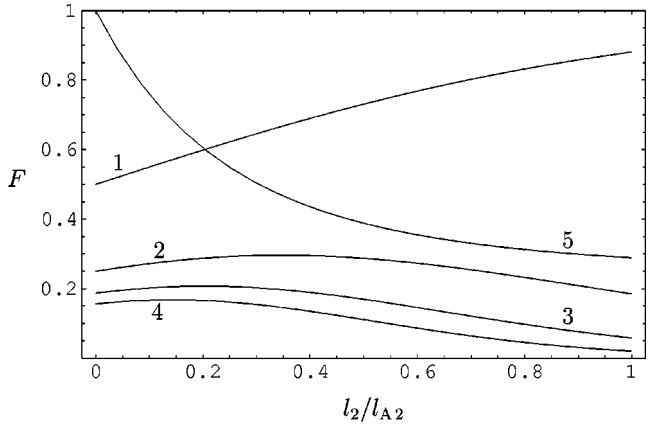

FIG. 6. The classical level ($\zeta=0$) of teleporting number states (curve 1: $N=0$; curve 2: $N=1$; curve 3: $N=2$; curve 4: $N=3$) and the corresponding average fidelity ($|\zeta|\to\infty$, curve 5) are shown as functions of the transmission length l_2 [$l_1=0$, $\tilde{\varphi}=0$, $\lambda=|T_2/T_1|=\exp(-l_2/l_{A2})$].

To overcome the problem of fast entanglement degradation of the TMSV, one could think about application of appropriate purification of Gaussian continuous-variable quantum states. Unfortunately a practically realizable purification scheme that compensates for the entanglement degradation of the TMSV has not been known so far. The purification protocol proposed in [25] enables one to distill maximally entangled states from a mixed two-mode entangled Gaussian state, but these states would be far from a TMSV needed for the teleportation scheme under consideration. In fact, the distilled states live in finite-dimensional Hilbert spaces. Even if they could be used in some modified teleportation scheme, the dimension of the Hilbert space should be sufficiently high. However, since the distillation probability exponentially decreases with the Hilbert-space dimension, one would effectively be left with the starting problem.

Throughout this paper we have restricted our attention to (quasi-) monochromatic fields. Using wave packets, the ultimate limits of quantum teleportation are not only determined by absorption but also by dispersion. Due to dispersion, the two wave packets unavoidably change their forms during propagation over longer distances, and the problem of mode mismatching in Alice's homodyne measurement and Bob's coherent displacement appears. The corresponding quantum efficiencies diminish, and hence the width of the Gaussian with which the Wigner function of the original quantum state is convolved is effectively increased. As a result, the teleportation fidelity is reduced. It can be expected that the effect sensitively depends on the position of the source of the

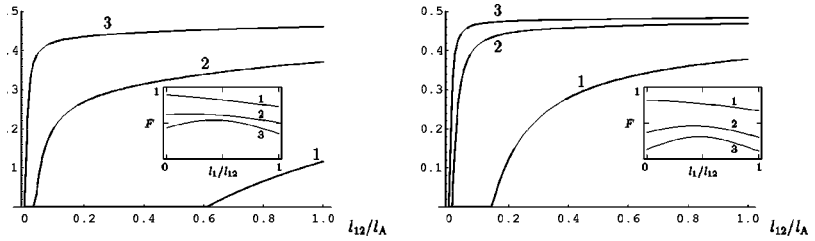

FIG. 7. The optimal distance l_1 from Alice to the position of an infinitely squeezed TMSV, for which maximum teleportation fidelity is realized, is shown as a function of the teleportation distance $l_{12}=l_1+l_2$ ($\tilde{\varphi}=0$, $\lambda=|T_2/T_1|=\exp[(l_1-l_2)/l_A]$) for (a) squeezed states (curve 1: $\zeta_0=0.78$, $\alpha_0=0.5$, i.e., $\bar{n}\approx 1$; curve 2: $\zeta_0=1.44$, $\alpha_0=1$, i.e., $\bar{n}\approx 5$; curve 3: $\zeta_0=1.63$, $\alpha_0=2$, i.e., $\bar{n}\approx 10$) and (b) number states (curve 1: $N=1$; curve 2: $N=5$; curve 3: $N=10$). The insets show the dependence of the fidelity on the position of the source of the TMSV for $l_{12}/l_A=0.1$.

TMSV. In order to understand the details, a separate analysis is required, which will be given elsewhere.

ACKNOWLEDGMENTS

This work was supported by the Deutsche Forschungsgemeinschaft, the RFBR-BRFBR Grant No. 00-02-81023 Bel2000_a, and the Heisenberg-Landau Program. One of us (D.G.W.) would like to acknowledge discussions with M. S. Kim.

APPENDIX: GAUSSIAN STATES

Let us consider the Gaussian Wigner function

$$W_{\rm in}(\gamma)=\frac{N_{\rm in}}{\pi}\exp(-A_{\rm in}|\gamma|^2-B_{\rm in}\gamma^{*2}-B_{\rm in}^{*}\gamma^2+C_{\rm in}\gamma^{*}+C_{\rm in}^{*}\gamma-D_{\rm in}), \tag{A1}$$

where

$$N_{\rm in}=\sqrt{A_{\rm in}^2-4|B_{\rm in}|^2}, \tag{A2}$$

$$D_{\rm in}=\frac{1}{N_{\rm in}^2}[A_{\rm in}|C_{\rm in}|^2-(B_{\rm in}^{*}C_{\rm in}^2+B_{\rm in}C_{\rm in}^{*2})]. \tag{A3}$$

Here, $C_{\rm in}$ can be chosen freely, and $A_{\rm in}$ and $B_{\rm in}$ must be chosen such that the condition $A_{\rm in}>2|B_{\rm in}|$ is satisfied. Substituting Eq. (A1) into Eq. (22) and performing the integration, we again obtain a Gaussian:

$$W_{\rm out}(\beta)=\frac{N_{\rm out}}{\pi}\exp(-A_{\rm out}|\beta|^2-B_{\rm out}\beta^{*2}-B_{\rm out}^{*}\beta^2+C_{\rm out}\beta^{*}+C_{\rm out}^{*}\beta-D_{\rm out}) \tag{A4}$$

($\tilde{\varphi}=0$), where

$$A_{\rm out}=\frac{1}{4(\lambda\sigma)^2}\left[2\sigma-\frac{A_{\rm in}+1/(2\sigma)}{[A_{\rm in}+(1/2\sigma)]^2-4|B_{\rm in}|^2}\right], \tag{A5}$$

$$B_{\rm out}=\frac{1}{4(\lambda\sigma)^2}\frac{B_{\rm in}}{[A_{\rm in}+1/(2\sigma)]^2-4|B_{\rm in}|^2}, \tag{A6}$$

$$C_{\rm out}=\frac{1}{2\lambda\sigma}\frac{[A_{\rm in}+1/(2\sigma)]C_{\rm in}-2B_{\rm in}C_{\rm in}^{*}}{[A_{\rm in}+1/(2\sigma)]^2-4|B_{\rm in}|^2}, \tag{A7}$$

and $N_{\rm out}$ and $D_{\rm out}$ are given according to Eqs. (A2) and (A3), respectively, with the out quantities in place of the in quantities. The result is

$$N_{\rm out}=\frac{1}{2\lambda^2\sigma}\frac{N_{\rm in}}{\sqrt{[A_{\rm in}+1/(2\sigma)]^2-4|B_{\rm in}|^2}}, \tag{A8}$$

$$D_{\rm out}=D_{\rm in}-\frac{[A_{\rm in}+1/(2\sigma)]|C_{\rm in}|^2-(B_{\rm in}^{*}C_{\rm in}^2+B_{\rm in}C_{\rm in}^{*2})}{[A_{\rm in}+1/(2\sigma)]^2-4|B_{\rm in}|^2}. \tag{A9}$$

Specifying $A_{\rm in}$, $B_{\rm in}$, and $C_{\rm in}$ according to Eqs. (27)–(29), Eq. (A4) [together with Eqs.(A5)–(A9)], we arrive at Eq. (30) [together with Eqs. (31)–(34)].

Using Eqs. (A1) and (A4), it is not difficult to prove that

$$\pi\int d^2\beta W_{\rm in}(\beta)W_{\rm out}(\beta)=\frac{2N_{\rm out}}{\sqrt{A^2-4|B|^2}}\exp\left[\frac{A|C|^2-(B^{*}C^2+BC^{*2})}{A^2-4|B|^2}-D\right], \tag{A10}$$

where

$$A=A_{\rm in}+A_{\rm out}, \tag{A11}$$

$$B=B_{\rm in}+B_{\rm out}, \tag{A12}$$

$$C=C_{\rm in}+C_{\rm out}, \tag{A13}$$

$$D=D_{\rm in}+D_{\rm out}. \tag{A14}$$

The above-mentioned specification of $A_{\rm in}$, $B_{\rm in}$, and $C_{\rm in}$ then leads to Eq. (35) [together with Eq. (36)].

[1] C. H. Bennett, G. Brassard, C. Crepeau, R. Jozsa, A. Peres, and W. K. Wooters, Phys. Rev. Lett. **70**, 1895 (1993).
[2] S. Stenholm and P. J. Bardroff, Phys. Rev. A **58**, 4373 (1998).
[3] L. Vaidman, Phys. Rev. A **49**, 1473 (1994).
[4] S. L. Braunstein and H. J. Kimble, Phys. Rev. Lett. **80**, 869 (1998).
[5] G. J. Milburn and S. L. Braunstein, Phys. Rev. A **60**, 937 (1999).
[6] D. B. Horoshko and S. Ya. Kilin, Phys. Rev. A **61**, 032304 (2000).
[7] P. van Loock, S. L. Braunstein, and H. J. Kimble, Phys. Rev. A **62**, 022309 (2000).
[8] J. Clausen, T. Opatrný, and D.-G. Welsch, Phys. Rev. A **62**, 042308 (2000).
[9] D. Bouwmeester, J.-W. Pan, K. Mattle, M. Eibl, H. Weinfurter, and A. Zeilinger, Nature (London) **390**, 575 (1997).
[10] D. Boschi, S. Branca, F. De Martini, L. Hardy, and S. Popescu, Phys. Rev. Lett. **80**, 1121 (1998).
[11] T. C. Ralph and P. K. Lam, Phys. Rev. Lett. **81**, 5668 (1998).
[12] A. Furusawa, J. L. Sørensen, S. L. Braunstein, C. A. Fuchs, H. J. Kimble, and E. S. Polzig, Science **282**, 706 (1998).
[13] L.-M. Duan and G.-C. Guo, Quantum Semiclassic. Opt. **9**, 953 (1997).
[14] S. Scheel, L. Knöll, T. Opatrný, and D.-G. Welsch, Phys. Rev. A **62**, 043803 (2000).
[15] S. Scheel, T. Opatrný, and D.-G. Welsch, International Conference on Quantum Optics 2000, Raubichi, 2000; e-print quant-ph/0006026.
[16] J. Lee, M. S. Kim, and H. Jeong, Phys. Rev. A **62**, 032305 (2000).
[17] S. Scheel and D.-G. Welsch, Phys. Rev. A (to be published).
[18] A. V. Chizhov, E. Schmidt, L. Knöll, and D.-G. Welsch, J. Opt. B: Quantum Semiclassical Opt. **3**, 77 (2001).
[19] T. Gruner and D.-G. Welsch, Phys. Rev. A **54**, 1661 (1996).
[20] L. Knöll, S. Scheel, E. Schmidt, D.-G. Welsch, and A. V. Chizhov, Phys. Rev. A **59**, 4716 (1999).
[21] K. E. Cahill and R. J. Glauber, Phys. Rev. **177**, 1857 (1969).
[22] K. E. Cahill and R. J. Glauber, Phys. Rev. **177**, 1882 (1969).
[23] *Handbook of Mathematical Functions*, edited by M. Abramowitz and I. Stegun (Dover, New York, 1970).
[24] M. S. Kim and J. Lee, Phys. Rev. A **64**, 012309 (2001).
[25] L.-M. Duan, G. Giedke, J. I. Cirac, and P. Zoller, Phys. Rev. Lett. **84**, 4002 (2000).